

Multistage nucleation of two-dimensional Si islands on Si(111)-7×7 during MBE growth: STM experiments and extended rate-equation model

Sergey Filimonov,^{1,2,*} Vasily Cherepanov,² Yuri Hervieu,¹ and Bert Voigtländer²¹*Department of Physics, Tomsk State University, Tomsk 634050, Russia*²*Institute of Bio- and Nanosystems (IBN 3) and cni – Center of Nanoelectronic Systems for Information Technology, Research Center Jülich, 52425 Jülich, Germany*

(Received 30 March 2007; published 23 July 2007)

The submonolayer density of two-dimensional (2D) islands in Si/Si(111)-7×7 molecular beam epitaxy is measured using scanning tunneling microscopy. At a relatively low deposition temperature of 673 K, the density of 2D islands is a power function of the deposition flux $N_{2D} \propto F^\chi$ with the exponent $\chi=0.24$ being smaller than that predicted by the standard nucleation theory. The nonstandard scaling of the 2D island density is explained by the multistage character of the nucleation process on the Si(111)-7×7 surface which involves consecutive stages of formation of stable Si clusters, formation of pairs of clusters, and transformation of the cluster pairs to 2D islands. Using an extended rate-equation model, we analyze the temperature and growth rate dependencies of the density of single clusters, cluster pairs, and 2D islands and show that an activation barrier of ~ 1.26 eV delays the transformation of cluster pairs to 2D islands. The delayed transformation of cluster pairs to 2D islands is the reason for the nonstandard scaling of the 2D island density observed at low deposition temperatures.

DOI: [10.1103/PhysRevB.76.035428](https://doi.org/10.1103/PhysRevB.76.035428)

PACS number(s): 68.55.Ac, 68.47.Fg, 81.15.Aa, 81.15.Hi

I. INTRODUCTION

The nucleation of two-dimensional (2D) islands in submonolayer epitaxial growth attracts considerable attention because of potential applications of the arrays of ultrasmall islands with high density in nanoelectronics.¹ On the other hand, the collective properties of island arrays, such as the density of 2D islands and their size distribution, are very sensitive to details of adatom hopping and bonding, thus making those fundamental processes in a certain sense accessible by the surface imaging techniques, e.g., by the scanning tunneling microscopy (STM).^{2–8}

The standard nucleation scenario,⁹ usually considered in the context of molecular beam epitaxy (MBE), includes random deposition of atoms on the surface followed by their random migration. Migrating adatoms meet each other and create clusters on the surface. It is assumed that there exists a critical cluster size i^* , such that clusters containing i^* and less atoms are unstable and most probably dissociate into adatoms with time. Clusters containing more than i^* atoms are assumed to be stable against dissociation and grow further by capturing migrating adatoms.^{10,11}

As can be seen, in this standard nucleation scenario, a cluster becomes a 2D island whenever its size exceeds the critical value i^* . This presumes correct *epitaxial* arrangement of atoms in the critical cluster—an assumption which usually works well if the surface atoms are kept in the bulklike positions but may often be wrong if the surface is reconstructed.¹² For instance, the Si(111) surface is characterized by a very stable and complicated (7×7) surface reconstruction. The (7×7) reconstruction unit cell consists of two triangular subunits. In the unfaulted half unit cell (HUC), the stacking sequence corresponds to the normal (bulk) stacking, while the layers in the faulted HUC form a stacking fault with respect to the bulk.¹³ Due to the presence of the reconstruction, it is expected that the nucleation of 2D

islands does not follow the simple scenario described in the previous paragraph.

At typical growth temperatures (600–900 K), submonolayer deposition of silicon on the Si(111)-7×7 surface results in the formation of two types of objects: small clusters occupying the half unit cells of the surface reconstruction and 2D islands that extend over plural HUCs.¹⁴ Small clusters have a height of $\sim 1/3$ of the step height on Si(111) and show no epitaxial arrangement of the constituting atoms.¹⁵ On the contrary, the height of 2D islands equals to the step height and the characteristic reconstruction pattern can be seen in high resolution STM images.^{14,15} Another important property distinguishing small clusters from 2D islands is that small clusters do not grow above a limiting size¹⁶ of about eight atoms.^{17,18} To emphasize an enhanced stability of small clusters on Si(111)-7×7, they are sometimes called “magic” clusters.¹⁹

Evidently, the presence of these clusters which on a certain time scale neither grow nor decay may substantially modify the nucleation kinetics. Since the formation of a cluster leaves the surface reconstruction intact, it is easier to form a cluster than a 2D island. So, the onset of the 2D nucleation may be delayed due to accumulation of adatoms to small clusters. On the other hand, the material accumulated in the clusters may assist otherwise impeded reconstruction removal.^{20,21}

A plausible scenario of the nucleation process on Si(111)-7×7 was proposed by Tochihara and Shimada.²⁰ According to Ref. 20, the nucleation of a 2D island on Si(111)-7×7 involves formation of a group of three clusters in neighboring half unit cells followed by their coalescence with simultaneous conversion of the stacking fault underneath the central cluster to the normal stacking. This coalescence-destruction mechanism was treated on a more quantitative level by Thibaudau²² who derived an expression for the density of 2D islands as a function of the growth

temperature and deposition rate. However, the three clusters involved into the nucleation were considered as an entity in Ref. 22, which appears to be a rather crude approximation bearing in mind the experimental observations available.

For instance, recently, we have shown that the nucleation of a 2D Si island on Si(111)-7×7 predominantly proceeds via formation of a critical nucleus consisting of a pair of clusters sitting in two halves of the same unit cell plus a certain number of additional adatoms loosely bonded to the clusters.²³ The small clusters constituting the cluster pair form one by one, so that the 2D nucleation represents a *multistage* process. In the present paper, the mechanism of 2D nucleation on Si(111)-7×7 is explored in more detail using STM experiments and a rate-equation theory. It is shown that the submonolayer density of 2D Si islands on Si(111)-7×7 obeys a power-law dependence on the deposition flux $N_{2D} \propto F^\chi$ with the scaling exponent $\chi=0.24$ being smaller than the smallest value allowed by the standard nucleation theory.^{10,11} To explain this nonstandard scaling of the 2D island density, an extended rate-equation model is proposed. The model takes into account the multistage character of the nucleation process on the Si(111)-7×7 surface and allows a unified description of the densities of small clusters and 2D islands. With this model, we obtain a set of scaling exponents for small clusters, cluster pairs, and 2D islands in the different regimes of growth and show that the accumulation of cluster pairs due to their delayed transformation to 2D islands may be responsible for the nonstandard scaling of the 2D island density observed in the experiment.

II. EXPERIMENT

Experiments were performed in an ultrahigh vacuum chamber with a base pressure less than 3×10^{-11} mbar. The clean defect-free Si(111)-7×7 surface was prepared by *in situ* annealing at 1500 K and slow cooling down to the growth temperature. The temperature of the substrate was measured using an infrared pyrometer. As a source of Si, an evaporator with a tantalum crucible heated by electron bombardment was used. The deposition flux was controlled by a quartz crystal balance monitor and using the coverage estimated from the STM images. The STM images were taken at room temperature in the constant current mode at a sample bias voltage between +2 and -2 V and tunneling current of 0.1 nA.

A. Nucleation mechanism

Small Si clusters and 2D Si islands were created on Si(111)-7×7 by deposition of 0.2 BL (bilayer) Si (1 BL = 1.56×10^{15} atoms/cm²). An example of the surface morphology after deposition of 0.2 BL Si at $T=680$ K and $F=0.4$ BL/min is shown in Fig. 1(a). In accordance with our earlier observations, three types of objects can be identified on the surface:²³ 2D islands, single clusters, and cluster pairs [see Fig. 1(a)]. Cluster pairs could also be seen in the STM images obtained by other authors.^{15,16,24} One should emphasize that pairs of clusters are present at the surface at a density larger than one would expect if they were created by a

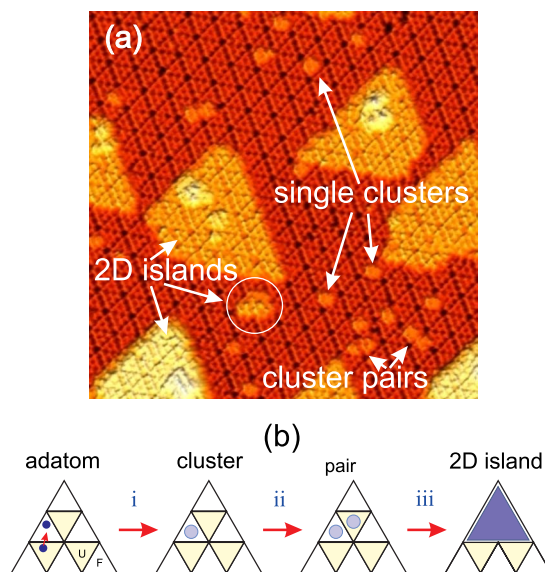


FIG. 1. (Color online) (a) STM image of the Si(111)-7×7 surface after deposition of 0.2 BL Si at a rate of 0.2 BL/min and temperature of 680 K. The image size is $425 \times 425 \text{ \AA}^2$. Three types of objects can be seen: 2D islands, single clusters, and cluster pairs. The smallest 2D island marked by a circle has a size of one unit cell. (b) Multistage nucleation pathway on Si(111)-7×7: (i) migrating adatoms form single clusters, (ii) single clusters stimulate appearance of cluster pairs, and (iii) the pairs transform to 2D islands.

random allocation of single clusters. For instance, at $T=613-680$ K and $F=0.4$ BL/min, the measured density of cluster pairs is two to four times higher than expected for random distribution of clusters on the surface (see Ref. 23 for details). This shows that a preference in the filling of a half unit cell exists nearby a HUC already occupied by a cluster.

The smallest 2D island observed by STM [marked by a circle in Fig. 1(a)] has a size of one unit cell of the (7×7) reconstruction. The assignment of this island as a 2D island is obtained by its height and by the observation of adatoms with the characteristic reconstruction signature. Together with the preferred formation of cluster pairs, this suggests that the nucleation of a 2D Si island on Si(111)-7×7 is a multistage process that includes (i) formation of a stable cluster in an unoccupied HUC, (ii) formation of the second stable cluster in a neighboring HUC of the same unit cell, and (iii) local reconstruction removal and transformation of the cluster pair to a 2D island [see Fig. 1(b)].

An important property of this multistage nucleation scenario is that intermediate products of the nucleation “reaction” are stable objects. To assess the time scale on which small Si clusters do not decay, one may refer to the STM experiments of Hwang *et al.*¹⁹ who observed the motion of small Si clusters on the Si(111)-7×7 surface. The residence time of a cluster in a half unit cell was about 120 s at $T=723$ K.¹⁹ Although it is not clear whether the cluster motion was due to the cluster decomposition followed by their reintegration or, as claimed in Ref. 19, clusters perform long jumps, one may conclude that at $T=723$ K, the clusters neither decay nor migrate, at least on the time scale of 120 s.

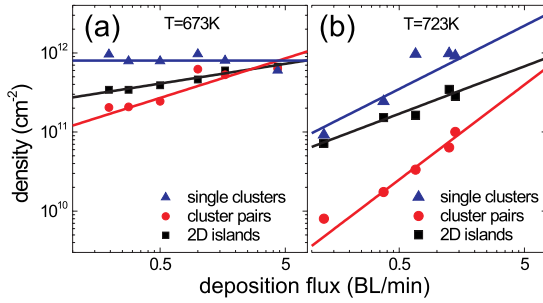


FIG. 2. (Color online) Flux dependence of the density of single clusters (triangles), cluster pairs (circles), and 2D islands (squares). (a) At a relatively low deposition temperature of 673 K, a power-law behavior of the density of 2D islands with a surprisingly low slope $\chi=0.24\pm 0.03$ is observed. (b) At $T=723$ K, linear regression gives $\chi=0.6\pm 0.1$ which is within the limits of the standard nucleation theory. Solid lines in (a) and (b) are the best fits to the experimental data obtained with an extended rate-equation model (see text for details).

Therefore, the clusters observed in our experiments ($T \leq 723$ K, deposition time shorter than 60 s) can be considered as stable objects.

B. Density of 2D islands and small clusters

Valuable information regarding the mechanism of 2D island nucleation can be gained from an analysis of the density of 2D islands N_{2D} as a function of the deposition flux F . For instance, measuring the $N_{2D}(F)$ dependence, one could check whether the nucleation process follows the standard nucleation scenario or not. The standard nucleation theory^{10,11} predicts a power-law scaling of the saturation density of 2D islands with the deposition flux: $N_{2D} \sim F^\chi$, where $\chi = i^*/(i^* + 2)$ varies from $1/3$ at $i^* = 1$ to 1 in the limit of large critical sizes. Any value of χ beyond this interval would indicate that the nucleation process is more complicated than that considered by the standard model.

The flux dependencies of the densities of 2D islands, single clusters, and cluster pairs on Si(111)- 7×7 were measured at two growth temperatures (Fig. 2). The experiment shows that the density of 2D islands is indeed a power function of the deposition flux F . However, at a relatively low temperature of 673 K, the measured scaling exponent $\chi = 0.24 \pm 0.03$ is smaller than the smallest value of $1/3$ predicted by the standard nucleation theory [Fig. 2(a)],^{10,11} whereas measurements at a higher temperature of 723 K yield the scaling exponent $\chi = 0.6 \pm 0.1$ which is within the limits of the standard model. As will be shown later, the nonstandard scaling observed at $T=673$ K results from the multistage character of the nucleation process.

The densities of single clusters n_s and cluster pairs n_p could also be approximated by power-law dependencies such as $n_s \sim F^\beta$ and $n_p \sim F^\gamma$. The fit of the experimental data yields $\beta = -0.1 \pm 0.1$ and $\gamma = 0.44 \pm 0.1$ at $T=673$ K ($\beta = 0.7 \pm 0.1$ and $\gamma = 1.2 \pm 0.3$ at $T=723$ K). As can be seen, the flux dependence of the density of cluster pairs is characterized by a larger slope than similar dependencies for single clusters and 2D islands. Interestingly, both at low and high temperatures,

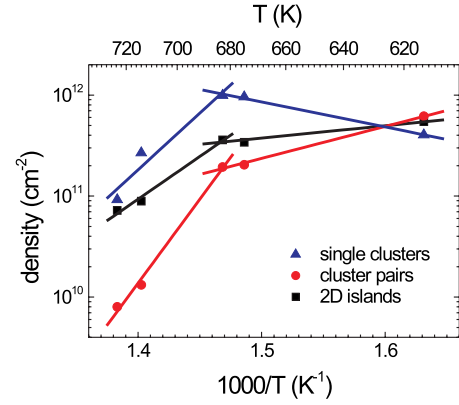


FIG. 3. (Color online) Arrhenius plot of the density of single clusters (triangles), cluster pairs (circles), and 2D islands (squares) measured at a coverage of 0.2 BL and deposition flux $F = 0.2$ BL/min. Symbols, experiment; solid lines, linear regression to the experimental data.

γ is about two times larger than χ . The relation between γ and β seems to be more complicated.

The temperature dependencies of the densities of single clusters, cluster pairs, and 2D islands also demonstrate different behavior at low and high T . As can be seen from Fig. 3 at the lower end of the explored temperature range, i.e., for $613 \text{ K} < T < 680 \text{ K}$, the Arrhenius plots of n_s , n_p , and N_{2D} are characterized by smaller slopes than at higher temperatures. From the low- T part of the plot ($613 \text{ K} < T < 680 \text{ K}$), the following estimates for characteristic energies of the formation of single clusters, cluster pairs, and 2D islands are obtained: $E_s = -0.49 \pm 0.03$ eV, $E_p = 0.63 \pm 0.04$ eV, and $E_{2D} = 0.24 \pm 0.05$ eV. Interestingly, for single clusters, not only the absolute value but also the sign of the slope changes: at low T , the density of small clusters n_s is an increasing function of the growth temperature. It will be shown below that this untypical behavior is also related to the multistage mechanism of the 2D nucleation on Si(111)- 7×7 .

III. MODEL

A. Rate equations

The analysis of rate equations is known to be a powerful tool to study scaling of the submonolayer island density with the deposition flux and growth temperature. Here, we propose a minimal rate-equation model that captures the multistage character of the 2D Si nucleation on Si(111)- 7×7 . It is assumed that the nucleation of a 2D Si island on Si(111)- 7×7 proceeds in the following three steps shown in Fig. 1(b): (i) a stable cluster forms in an unoccupied HUC, (ii) the second stable cluster appears in the neighboring HUC of the same unit cell, (iii) the reconstruction is locally lifted in the unit cell occupied by the cluster pair and the pair transforms to a 2D island. This multistage nucleation mechanism can be described quantitatively by the following set of rate equations for the densities of adatoms n_1 , single clusters n_s , cluster pairs n_p , and 2D islands N_{2D} ,

$$\frac{dn_1}{dt} = F - G^* - G, \quad (1)$$

$$\frac{dn_s}{dt} = J_s - J_p, \quad (2)$$

$$\frac{dn_p}{dt} = J_p - J_{2D}, \quad (3)$$

$$\frac{dN_{2D}}{dt} = J_{2D}. \quad (4)$$

Here, G is the flux of adatoms incorporating into the 2D islands: $G = \sigma_{av} D n_1 N_{2D}$, where σ_{av} is the average capture number of the 2D islands^{10,11} and $D = \nu \exp(-E_d/k_B T)$ is the surface diffusion coefficient ($\nu = 10^{13} \text{ s}^{-1}$ is the attempt frequency, E_d is the adatom diffusion barrier, and k_B is the Boltzmann constant). The flux G^* describes accumulation of adatoms in single clusters and cluster pairs together with the consumption of adatoms in course of the transformation of the cluster pairs into 2D islands. J_s , J_p , and J_{2D} are the rates of formation of single clusters, cluster pairs, and 2D islands, respectively. This set of equations extends the rate equations used in the standard nucleation models^{10,11} by including Eqs. (2) and (3) which describe the birth and death of stable single clusters and cluster pairs.

The cluster formation rate J_s is calculated in the standard way using the critical nucleus approximation.^{10,11} If i is the size of the critical nucleus to form a stable cluster, then

$$J_s = \sigma_i D e^{E_i/k_B T} n_1^{i+1}, \quad (5)$$

where E_i is the energy to dissociate the nucleus into single adatoms and σ_i is the capture number.

The formation of cluster pairs represents a heterogeneous process where single clusters serve as the nucleation centers for the pairs. Therefore, the rate of pair formation must be proportional to the density of single clusters n_s . Assuming that the formation of the stable cluster nearby an already occupied HUC proceeds through the formation of the critical nucleus of size j , one writes

$$J_p = \sigma_j D e^{E_j/k_B T} n_1^{j+1} n_s. \quad (6)$$

It should be noted that the critical sizes i and j , as well as the dissociation energies E_i and E_j , may be different. Moreover, even when $i=j$, the dissociation energies are not necessarily equal because the presence of a cluster in a HUC may modify the bonding configuration in the neighboring HUCs, e.g., by a charge transfer to the cluster.²⁵ Also, a kind of nonlocal attractive interaction between clusters and adatoms could exist, like in the case of metal clusters on Si(111)- 7×7 .^{26,27}

Like single clusters are precursors for cluster pairs, the pairs are precursors for 2D islands. However, the transformation of a cluster pair to a 2D island requires not only accu-

mulation of additional atoms but also a structural transformation involving both the atoms constituting the clusters and atoms belonging to the surface. The atomic scale details of this process are not really clear at the moment, but one may expect that there is an energy barrier that must be surmounted in order to launch the transformation. Applying again the concept of critical nucleus, we write down the nucleation rate as

$$J_{2D} = \sigma_k D e^{E_k/k_B T} n_1^{k+1} n_p. \quad (7)$$

Here, σ_k is the corresponding capture number, and $k+1$ is the number of *additional* atoms which have to be accumulated by the cluster pair to make the pair-to-2D island transformation possible. The activation barrier (additional to E_d) that must be surmounted to start the transformation process is included into the parameter E_k which also contains the contribution from the dissociation energy of the critical nucleus.

B. Scaling relations

We are searching for the solutions of rate equations (1)–(4) which allow the power-law scaling of the densities of single clusters, pairs, and 2D islands with the deposition flux and the Arrhenius dependence on the growth temperature:

$$n_s \sim F^\beta e^{E_s/k_B T}, \quad (8)$$

$$n_p \sim F^\gamma e^{E_p/k_B T}, \quad (9)$$

$$N_{2D} \sim F^\chi e^{E_{2D}/k_B T}. \quad (10)$$

Here, E_s , E_p , and E_{2D} are the characteristic energies of the formation of single clusters, pairs, and 2D islands, respectively. We replace time t in Eqs. (1)–(4) by the surface coverage $\theta = Ft$ and treat θ as the independent variable.¹⁰ Then, we consider the steady-state stage of growth when atoms entering the surface from the molecular beam incorporate, for the most part, into the edges of 2D islands.^{10,11} In this case, $n_1 \approx F/\sigma_{av} D N_{2D}$ and the scaling relations (8)–(10) take place in the four regimes of nucleation, as listed below (see Fig. 4). Mathematically, each of these four regimes represents a particular case of the rate equations where the second term in the right part of Eqs. (2) and (3) is either neglected or put equal to the first term. In these cases, the scaling exponents and the relations among the characteristic energies might be found using simple algebra after substitution of Eqs. (8)–(10) into the rate equations.

Regime I is the steady-state regime of nucleation when the formation of single clusters is balanced by their transformation to cluster pairs ($J_s \approx J_p$) and the formation of the cluster pairs is balanced by their transformation to 2D islands ($J_p \approx J_{2D}$). In this regime, the 2D nucleation rate occurs to be

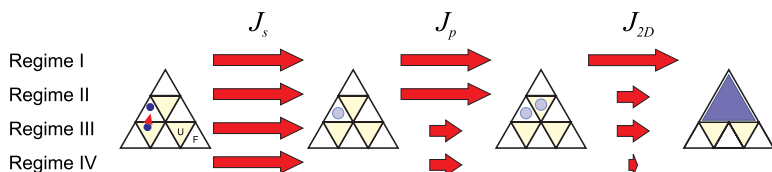


FIG. 4. (Color online) Four regimes of nucleation of 2D Si islands on the Si(111)- 7×7 surface. Short arrows mark slow nucleation stages.

TABLE I. Scaling exponents and characteristic energies.

| | β | γ | χ | E_i+iE_d | E_j+jE_d | E_k+kE_d |
|------------|--------------------------|---------------------------|-------------------------|-------------------|-----------------------|-------------------|
| Regime I | $2 \frac{i-j}{i+2}$ | $2 \frac{i-k}{i+2}$ | $\frac{i}{i+2}$ | $(i+2)E_{2D}$ | $(j+2)E_{2D}-E_s$ | |
| Regime II | $3 \frac{i-j}{i+k+3}$ | $\frac{2i-k}{i+k+3}$ | $\frac{i+k}{i+k+3}$ | $(i+1)E_{2D}+E_p$ | $(j+1)E_{2D}+E_p-E_s$ | $(k+2)E_{2D}-E_p$ |
| Regime III | $\frac{2i-j}{i+j+3}$ | $\frac{2i+2j-3k}{i+j+3}$ | $\frac{i+j}{i+j+3}$ | $(i+1)E_{2D}+E_s$ | $(j+2)E_{2D}-E_s$ | |
| Regime IV | $\frac{3i-j-k}{i+j+k+4}$ | $2 \frac{i+j-k}{i+j+k+4}$ | $\frac{i+j+k}{i+j+k+4}$ | $(i+1)E_{2D}+E_s$ | $(j+1)E_{2D}+E_p-E_s$ | |

equal to the rate of formation of the smallest stable cluster (single cluster), so that the presence of any intermediate stable objects (e.g., cluster pairs) does not affect the scaling of the 2D island density and the scaling exponent χ has its canonical form $\chi=i/(i+2)$.

In regime II, the formation of single clusters is balanced by their transformation to cluster pairs ($J_s \approx J_p$), but the transformation of the cluster pairs to 2D islands is strongly delayed, e.g., due to the high activation barrier for reconstruction removal. In this case $J_p \gg J_{2D}$, and accumulation of cluster pairs takes place. This yields a nonstandard scaling of the 2D island density with $\chi=(i+k)/(i+k+3)$. Thus, the scaling exponent χ in regime II depends not only on the size of the smallest critical nucleus i but also on k , i.e., on the number of additional atoms which a cluster pair must accumulate to launch its transformation to a 2D island.

Regime III represents an opposite case when the pairs easily transform to 2D islands ($J_p \approx J_{2D}$) but single clusters accumulate at the surface due to their delayed transformation to cluster pairs ($J_s \gg J_p$). This regime is characterized by the scaling exponent $\chi=(i+j)/(i+j+3)$.

Regime IV is the regime where both the pair formation and their transformation to 2D islands are delayed in comparison with the formation of single clusters ($J_s \gg J_p \gg J_{2D}$). This nucleation regime also results in a nonstandard scaling of the 2D island density: $\chi=(i+j+k)/(i+j+k+4)$.

The full set of the scaling exponents, including those for single clusters and cluster pairs, is given in the first half of Table I. The second half of the table contains the dissociation energies E_i , E_j , E_k , and the adatom diffusion barrier E_d expressed through the experimentally measurable characteristic energies E_s , E_p , and E_{2D} .

IV. DISCUSSION

In order to apply the developed model for a quantitative analysis of the data presented in Figs. 2 and 3, one has to ascertain first which of the four nucleation regimes is realized in the experiment. Since, as we will see later, an unambiguous identification of the nucleation regime at high deposition temperatures is hardly possible, we will concentrate on the data obtained at $613 \text{ K} < T < 680 \text{ K}$, i.e., at the lower end of the explored temperature range.

The signature of the low temperature nucleation regime in our experiments is the surprisingly low scaling exponent of 2D islands ($\chi=0.24 \pm 0.03$). Also, the density of single clusters demonstrates a very weak flux dependence ($\beta=-0.1 \pm 0.1$). Those two observations unambiguously identify the nucleation regime in our low- T experiments as regime II. As can be seen from Table I, the best fit to the experimental dependencies in Fig. 2(a) is achieved in the regime II with $i=j=1$ and $k=0$. This set of parameters yields $\beta=0$, $\gamma=0.5$, and $\chi=0.25$ in good agreement with the experiment. As $i=j=1$, a dimer formed by two Si adatoms represents a stable nucleus both for formation of a single stable cluster and the second stable cluster in a neighboring HUC. The zero value of k indicates that only one additional atom is required to trigger the reconstruction removal beneath the cluster pair.

With the critical sizes known from the flux dependencies, one could use the temperature dependencies of the cluster and island densities to estimate the energy parameters of the nucleation process. As a consistency check, one can evaluate the barrier for surface diffusion E_d . Since the dimer is the stable nucleus for the single cluster ($i=1$), one has $E_i=0$ and a simple relation holds: $E_d=2E_{2D}+E_p$ (see Table I). Using $E_p=0.63 \text{ eV}$ and $E_{2D}=0.24 \text{ eV}$, as measured from the low- T part of Fig. 3, one gets $E_d=1.11 \text{ eV}$ which is in excellent agreement with the results of recent *ab initio* calculations²⁸ and an earlier experimental estimate obtained with the atom-tracking STM technique.²⁹ As can be seen from Table I, such a good agreement could not be achieved in regimes I, III, and IV.

Now, we estimate the dissociation energy E_j , which is the work to remove an unstable cluster of j atoms from the second half of a (7×7) unit cell already occupied by a stable single cluster. Since $j=1$, this parameter is a measure of the influence of a single Si cluster on the adatom bonding in the neighboring (empty) HUCs. Using the expression for E_j in regime II from Table I and the measured value of E_s , one obtains $E_j=-E_s=0.49 \text{ eV}$. This shows that the presence of a cluster in a HUC modifies the bonding configuration in the neighboring HUCs creating there traps for migrating adatoms. This explains naturally the experimentally observed trend for Si clusters to form pairs. It becomes also clear why at low T the density of single clusters increases with increasing growth temperature: when the temperature goes up, the

role of the trap nearby an occupied HUC decreases, so that at high T , less cluster pairs form and more single clusters stay on the surface.

Since $k=0$, only one additional atom is required to launch the transformation of the cluster pair to a 2D island. In this case, E_k is simply the difference between the surface diffusion barrier E_d and the activation barrier that must be surmounted to start the transformation process. Taking the measured values for E_{2D} and E_p , and the relevant expression from Table I, one gets $E_k=-0.15$ eV. Altogether, the difference $E_d-E_k=1.26$ eV represents an effective activation barrier for the transformation of the cluster pair plus one atom to a 2D island (an effective nucleation barrier). This barrier is the reason for delayed transformation of cluster pairs to 2D islands.

With the increasing growth temperature, overcoming of the nucleation barrier becomes more frequent and the rate of transformation of cluster pairs to 2D islands may become compatible with the pair formation rate ($J_{2D}\approx J_p$). Therefore, one would expect transition from regime II to regime I at higher T . This would result in an increase of the scaling exponent χ to the canonical value of $1/3$. A larger value of 0.6 observed in the experiment at $T=723$ K could be explained by an increase of the critical size i . The best fit to the experimental dependencies in Fig. 2(b) is achieved in regime I with $i=3$, $j=1$, and $k=0$. However, an unambiguous identification of the high- T nucleation regime is hardly possible, because for each of four nucleation regimes, one could find a set of i , j , and k which would yield the scaling exponents β , γ , and χ close to the experimentally measured values (see Table I).

The transition from regime II to I and vice versa could also be achieved at a fixed T by changing the deposition rate. At lower rates, the cluster pairs would have more time to overcome the nucleation barrier, so that their accumulation on the surface will be prevented and the nucleation will proceed in the steady-state regime I. For instance, a power-law behavior of the 2D island density with a slope of 0.75 was observed at a temperature of $T=683$ K and deposition rates below 0.07 BL/min, indicating the critical cluster size $i=6$.³

Finally, we note that the proposed nucleation mechanism could also be a property of the Ge/Si(111)- 7×7 system. Similar to the growth of Si on Si(111)- 7×7 , submonolayer deposition of Ge results in the formation of both small Ge

clusters and larger 2D Ge islands.^{30,31} However, further systematical studies are necessary to identify the key stages of the 2D nucleation of Ge on Si(111)- 7×7 .

V. SUMMARY

Using STM experiments and an extended rate-equation model, we have performed a detailed analysis of the mechanism of 2D nucleation at the early stages of Si/Si(111)- 7×7 MBE growth. We showed that the nucleation of a 2D island on Si(111)- 7×7 proceeds in three steps. First, a small stable cluster occupying a half unit cell of the (7×7) reconstruction is created. The presence of a cluster in a HUC increases the binding energy of adatoms in the neighboring HUCs by ~ 0.49 eV. This gives rise to the next stage of the nucleation process at which the second cluster forms within the same unit cell. As a result, the preferential formation of cluster pairs takes place. At low deposition temperatures ($T < 680$ K) and relatively high deposition rates ($F > 0.2$ BL/min), the Si dimer represents the stable nucleus both for the formation of the single stable cluster and for the formation of the second stable cluster within the same unit cell. Third, after accumulation of a certain number of additional adatoms, the (7×7) reconstruction is locally removed and the cluster pair transforms to a 2D island. To launch the transformation of the cluster pair to the 2D island, one additional atom has to be attached to the cluster pair. The effective barrier for the pair-to-2D island transformation is estimated to be about ~ 1.26 eV. This barrier delays the transformation of cluster pairs to 2D islands at low T . Accumulation of the pairs due to their delayed transformation to 2D islands results in a nonstandard scaling of the submonolayer density of 2D islands with the scaling exponent $\chi = 0.24$ being smaller than that predicted by the standard nucleation theory.

ACKNOWLEDGMENTS

We thank Josef Mysliveček for fruitful discussions. This work was partially supported by INTAS under Grant No. 03-51-5015 (S.F. and Yu.H.), by the Russian Federal Agency for Science and Innovations under Grant No. MK-6647.2006.2 (S.F.), and by the Alexander von Humboldt Foundation (S.F.).

*filimon@phys.tsu.ru

¹V. A. Shchukin, N. N. Ledentsov, and D. Bimberg, *Epitaxy of Nanostructures* (Springer, Berlin, 2003).

²Y. W. Mo, J. Kleiner, M. B. Webb, and M. G. Lagally, *Phys. Rev. Lett.* **66**, 1998 (1991).

³B. Voigtländer and A. Zinner, *Surf. Sci.* **292**, L775 (1993).

⁴J. A. Strosio and D. T. Pierce, *Phys. Rev. B* **49**, R8522 (1994).

⁵B. Müller, L. Nedelmann, B. Fischer, H. Brune, and K. Kern, *Phys. Rev. B* **54**, 17858 (1996).

⁶H. Brune, G. S. Bales, J. Jacobsen, C. Boragno, and K. Kern,

Phys. Rev. B **60**, 5991 (1999).

⁷V. Cherepanov, S. Filimonov, J. Mysliveček, and B. Voigtländer, *Phys. Rev. B* **70**, 085401 (2004).

⁸H. Rauscher, J. Braun, and R. J. Behm, *Phys. Rev. Lett.* **96**, 116101 (2006).

⁹A. Pimpinelli and J. Villain, *Physics of Crystal Growth* (Cambridge University Press, Cambridge, 1998).

¹⁰J. A. Venables, G. D. T. Spiller, and M. Hanbücken, *Rep. Prog. Phys.* **47**, 399 (1984).

¹¹S. Stoyanov and D. Kashchiev, in *Current Topics in Material*

- Sciences*, edited by E. Kaldis (North-Holland, Amsterdam, 1981), Vol. 7, pp. 69–141.
- ¹²Raj Ganesh S. Pala and F. Liu, *Phys. Rev. Lett.* **95**, 136106 (2005).
- ¹³K. Takayanagi, Y. Tanishiro, S. Takahashi, and M. Takahashi, *Surf. Sci.* **164**, 367 (1985).
- ¹⁴U. Köhler, J. E. Demuth, and R. J. Hamers, *J. Vac. Sci. Technol. A* **7**, 2860 (1989).
- ¹⁵A. Ichimiya, T. Hashizume, K. Ishiyama, K. Motai, and T. Sakurai, *Ultramicroscopy* **42-44**, 910 (1992).
- ¹⁶T. Hasegawa, W. Shimada, H. Tochihara, and S. Hosoki, *J. Cryst. Growth* **166**, 314 (1996).
- ¹⁷H. Asaoka, V. Cherepanov, and B. Voigtländer, *Surf. Sci.* **588**, 19 (2005).
- ¹⁸F.-C. Chuang, B. Liu, C.-Z. Wang, T.-L. Chan, and K.-M. Ho, *Surf. Sci.* **598**, L339 (2005).
- ¹⁹I. S. Hwang, M. S. Ho, and T. T. Tsong, *Surf. Sci.* **514**, 309 (2002).
- ²⁰H. Tochihara and W. Shimada, *Surf. Sci.* **296**, 186 (1993).
- ²¹Y. Shigeta, *Surf. Rev. Lett.* **7**, 61 (2000).
- ²²F. Thibaudau, *Surf. Sci.* **416**, L1118 (1998).
- ²³S. N. Filimonov, V. Cherepanov, Yu. Yu. Hervieu, and B. Voigtländer, *Surf. Sci.* (to be published).
- ²⁴W. Shimada and H. Tochihara, *J. Cryst. Growth* **237-239**, 35 (2002).
- ²⁵H. F. Ma, Z. H. Qin, M. C. Xu, D. X. Shi, H.-J. Gao, S. Wang, and S. T. Pantelides, *Phys. Rev. B* **75**, 165403 (2007).
- ²⁶E. Vasco, C. Polop, and E. Rodríguez-Cañas, *Phys. Rev. B* **67**, 235412 (2003).
- ²⁷I. Ošt'ádal, P. Kocán, P. Sobotík, and J. Pudl, *Phys. Rev. Lett.* **95**, 146101 (2005).
- ²⁸C. M. Chang and C. M. Wei, *Phys. Rev. B* **67**, 033309 (2003).
- ²⁹T. Sato, S. Kitamura, and M. Iwatsuki, *J. Vac. Sci. Technol. A* **18**, 960 (2000).
- ³⁰M. Suzuki and Y. Shigeta, *Surf. Sci.* **539**, 113 (2003).
- ³¹S. A. Teys, A. B. Talochkin, K. N. Romanyuk, and B. Z. Olshansky, *Phys. Solid State* **46**, 80 (2004).